J MATER SCI **41** (2006) 4335–4341

Glycothermal synthesis of vanadium(III) phosphate hydrates

T. NAKAMURA, T. INUI, M. INOUE
Department of Energy and Hydrocarbon Chemistry, Graduate School of Engineering,
Kyoto University, Katsura, Kyoto 615-8510, Japan

T. MIYAKE*
Department of Chemical Engineering, Faculty of Engineering, Kansai University, 3-3-35
Yamate-cho, Suita 564-8680, Japan
E-mail: tmiyake@ipcku.kansai-u.ac.jp

Glycothermal reaction of various vanadium compounds with triethyl phosphate yielded two hydrate phases of vanadium(III) phosphate having tetragonal (Phase 1) and monoclinic (Phase 2) crystal systems, depending on the reaction conditions such as phosphorus/vanadium ratio, vanadium starting material, reaction temperature and solvent. Thermal treatment of Phase 2 in an anaerobic condition caused transformation to Phase 1 which finally transformed to VPO_4 through an intermediate phase (Phase M). Heat treatment of both the phases in an aerobic condition caused the formation of β-$VOPO_4$. *© 2006 Springer Science + Business Media, Inc.*

1. Introduction

To synthesize inorganic materials, many methods such as precipitation, co-precipitation, spray-drying, hydrothermal and alkoxide methods are known [1]. Among these methods, the hydrothermal synthesis uses water as a solvent and produces materials at higher temperatures than the boiling point of water. This method is often applied for the syntheses of crystalline inorganic compounds [2].

Recently, methods using organic solvents instead of water have been widely studied and syntheses of materials that cannot be obtained in water are reported such as silica-sodalite [3], $Ba[Al_2(C_2H_4O_2)_4]$ [4], and glycol derivative of boehmite [5].

One of the authors have developed use of glycol solvents in place of water for hydrothermal reaction [6–8] and this method was named as "glycothermal" one [9]. Adopting this method, α-alumina was obtained from fine particles of gibbsite [10] and yttrium-aluminum garnet (YAG) was synthesized from a stoichiometric mixture of yttrium acetate and aluminum isopropoxide [11, 12]. In these cases, the reaction proceeded under mild conditions; that is, lower temperatures and pressures than those required by hydrothermal reaction. 1,4-Butanediol is preferably used in the glycothermal reaction and this is construed as participation of the neighboring hydroxyl group of the intermediate glycoxide ($HO(CH_2)_4$–O–M<) to the scission of C–O bond [13], which dominates the overall reaction giving fine crystalline particles under mild conditions.

Vanadium is an important element in the field of oxidation catalysis [14]. For example, $(VO)_2P_2O_7$ is used as the catalyst to produce maleic anhydride from butane [15, 16]. Synthesis of $(VO)_2P_2O_7$ in alcohol such as n-butanol is reported and the choice of alcohol influences crystal habit of the produced $(VO)_2P_2O_7$ [17].

A variety of vanadium(III) phosphate have been reported so far: VPO_4 [18] and $V(PO_3)_3$ [19] were synthesized at high temperatures. $VPO_4{\cdot}H_2O$ and $V_{1.23}(PO_4)(OH)_{0.69}(H_2O)_{0.31}{\cdot}0.33H_2O$ were hydrothermally prepared by reduction of V_2O_5 with V metal in the presence of H_3PO_4 and organic amine [20]. $VPO_4{\cdot}2H_2O$ was prepared from V_2O_5 and H_3PO_4 in the presence of tripropyl amine, which acted as the reducing agent as well [21]. Another vanadium(III) phosphate phase, $H_3OVP_2O_7$ was prepared hydrothermally in the presence of tetraethyl ammonium chloride [22]. These vanadium(III) phosphates are also expected as a useful starting reagent for vanadium phosphate glasses or catalysts.

In this paper, the glycothermal synthesis of vanadium(III) phosphate was studied and the products were characterized in detail. As the glycol, 1,4-butanediol was mainly used.

---

*Author to whom all correspondence should be addressed.

0022-2461
DOI: 10.1007/s10853-006-7024-7

2. Experimental

2.1. Materials

Vanadium(III) acetylacetonate (hereafter the acetylacetonate group is abbreviated as acac) was purchased from Aldrich Chemicals. Vanadyl acetylacetonate, $VO(acac)_2$, was purchased from Dojin Chemical. $VOC_2O_4 \cdot nH_2O$ and NH_4VO_3 were purchased from Wako Pure Chemicals. V_2O_5 was purchased from Nacalai Tesque. Triethyl phosphate, $(EtO)_3PO$, was purchased from Wako Pure Chemicals. All of these reagents were used without further purification. 1,4-Butanediol (1,4-BG) was purchased from Nacalai Tesque.

2.2. Typical reaction procedure

Vanadyl acetylacetonate ($VO(acac)_2$; 5.0 g, 19 mmol) and a desired amount of $(EtO)_3PO$ were suspended in 100 cm^3 of 1,4-BG in a test tube serving as an autoclave liner, and the mixture was placed in a 300 cm^3 autoclave. An additional 30 cm^3 of 1,4-BG was placed in the gap between the autoclave wall and the test tube. The autoclave was completely purged with nitrogen, heated to the desired temperature (typically 315 °C) at a rate of 2.3 °C min^{-1}, and kept at this temperature for 2 h. During the reaction period, the autogeneous pressure gradually increased from 2 MPa to 3–14 MPa (depending on the reaction conditions) at the end of the reaction. After the assembly was cooled to room temperature, the resulting products were centrifuged. The products were repeatedly washed with acetone by vigorous stirring and centrifuging and thereafter dried in air.

2.3. Analyses

X-ray powder diffraction (XRD) was measured on a Shimadzu XD-D1 diffractometer using Cu $K\alpha$ radiation and a graphite monochromator. Average oxidation state of vanadium was measured according to the method reported by Hodnett et al. [23]. Water content in the reaction medium was analyzed by Karl-Fischer method. Simultaneous TG-DTA analyses were performed on a Shimadzu TG-30 thermal analyzer at a heating rate of 10 °C min^{-1} in a 40 cm^3 min^{-1} flow of dried nitrogen or 3.8% O_2–nitrogen. IR spectra were recorded on a Shimadzu IR-435 spectrophotometer.

3. Results

3.1. Synthesis of vanadium(III) phosphate hydrates

Varying the ratio of $(EtO)_3PO$ to $VO(acac)_2$ and treatment temperature, two products, Phase 1 and Phase 2, were obtained and their XRD patterns are shown in Fig. 1. The halo patterns around 2θ 10 to 15 degrees are from the grease used for XRD sample preparation. These patterns are essentially identical to those reported by Vaughey et al. [20], and Phase 1 can be assigned to tetragonal $V_{1+x}(PO_4)(OH)_{3x}(H_2O)_{1-x} \cdot nH_2O$ ($x = 0.23$, $n = 0.33$), while Phase 2, to monoclinic $VPO_4 \cdot H_2O$. The former phase was also prepared by Schindler et al. [24], and they gave the following formula; $V_{5.12}(PO_4)_4(OH)_{3.36}(H_2O)_{0.64} \cdot 0.84H_2O$. However, our product, Phase 1, seems to have a larger P/V ratio, which will be discussed later. Comparison of the unit cell parameters of the present products with those of the reported phases is shown in Table I. The average oxidation states of vanadium in Phase 1 and Phase 2 were measured by the method of Hodnett et al. [23] and were found to be 2.9 and 2.8, respectively. It must be noted that all of the hydrate phases of vanadium(III) phosphate reported so far were prepared by hydrothermal reaction in the presence of amine base or ammonium ion, and our result is the first example of the synthesis of vanadium(III) phosphate hydrates from the liquid phase in the absence of amines. The synthesis without amine is advantageous because the cost of the product would be reduced and at the same time NO_X would not be emitted on further treatment.

In Table II, the effects of the treatment conditions on the products are summarized. When the P/V ratio in the starting mixture was lower than 1.75, Phase 1 of yellow-green color appeared predominantly regardless of the temperatures studied. At higher P/V ratio between 2 and 3, Phase 2 of light green color appeared except the product obtained by the reaction at 250 C. For further high P/V ratio,

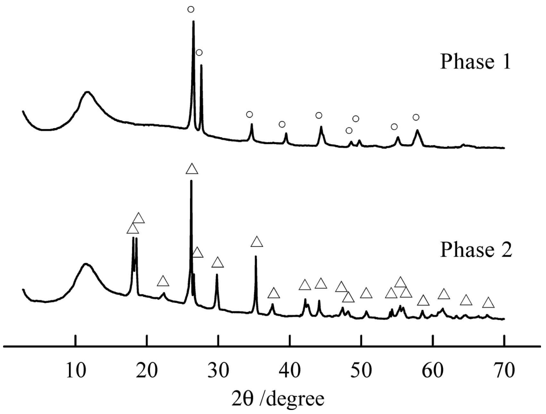

Figure 1 XRD patterns of vanadium phosphates obtained by the glycothermal method. (○; Phase 1, △; Phase 2).

TABLE I. Unit cell parameters

	Phase 1	$V_{1.23}(PO_4)(OH)_{0.69}$ $(H_2O)_{0.31} \cdot 0.33H_2O$	$V_{5.12}(PO_4)_4(OH)_{3.36}$ $(H_2O)_{0.64} \cdot 0.84H_2O$
a (Å)	5.156	5.1811	5.1646
b (Å)	13.03	12.9329	12.9217
V (Å^3)	346.39	347.17	344.66
	Phase 2	$VPO_4.H_2O$	
a (Å)	6.715	6.6954	
b (Å)	7.77	7.7925	
c (Å)	7.362	7.3504	
β (°)	115.18	115.255	

TABLE II. Influnce of P/V ratio and treatment temperature on products obtained by glycothermal treatment of $(EtO)_3PO$ and $VO(acac)_2$

Initial ratio (−) P : V	Treatment temperature (°C)	Phase
1:2	315	1
1:1	200	Amorphous
1:1	315	1
1.25:1	315	1
1.5:1	315	1
1.75:1	250	1
1.75:1	315	1
2:1	200	Amorphous
2:1	250	1
2:1	315	2
2.5:1	315	2
3:1	315	2
4:1	315	Amorphous

TABLE III. Influnce of oranic solvent on products

Oranic solvent	Phase
1,4-Butanediol (1,4-BG)	2
Ethylene glycol (EG)	1
20 wt% H_2O/EG	1
n-Propanol	1
Toluene	Amorphous

315 °C, $(EtO)_3PO:VO(acac)_2 = 2:1$.

the products were amorphous. These results indicate that the P/V ratio has an important role on the products obtained rather than the treatment temperature. When Phase 1 formed, the autogenous pressure was about 4 MPa. To the contrary, when Phase 2 formed, the autogenous pressure reached to about 14 MPa indicating that some 1,4-BG decomposed and released tetrahydrofuran and water both having lower boiling points.

3.2. Influence of solvent

Influence of organic solvents was studied and the results are indicated in Table III.

Only when 1,4-BG was used, Phase 2 was obtained. One possible explanation for these results may be that the presence of the large excess H_3PO_4 formed by hydrolysis of triethyl phosphate causes acid-catalyzed dehydration of 1,4-BG yielding tetrahydrofuran and water which facilitate the formation of Phase 2. To examine this possibility, water content after the reaction was analyzed. When 1,4-BG (initial content of water was 0.04 wt%) was used, the supernatant after the reaction contained 20.2 wt% water. This result indicates that the dehydration of 1,4-BG (i.e., formation of one mole of water from one mole of 1,4-BG) proceeded completely under the reaction conditions. On the other hand, when EG (initial water content, 0.08 wt%) was used, the water content in the supernatant after the reaction was 13.4 wt%. This result indicates that 92% of EG was dehydrated under the reaction condition, assuming the formation of diethylene glycol (i.e., one mole of water from two moles of EG). Therefore, EG is more thermally stable and lesser amount of water is present under the reaction conditions. However, intentional addition of water to the EG medium resulted in the formation of Phase 1 and thus water content in the reaction medium was not the cause of the formation of Phase 2 when 1,4-BG was used. In the case of the nonpolar solvent, toluene, an amorphous material formed. This result suggests that interaction between the solvent and the vanadium species and/or phosphate groups is a key factor to crystallize the products.

TABLE IV. Influence of starting vanadium compound on products

Starting vanadium compound	Phase
$V(acac)_3$	2
$VO(acac)_2$	2
VOC_2O_4	2
V_2O_5	2
NH_4VO_3	Unknown

315 °C, 1,4-BG, $(EtO)_3PO:V = 2:1$.

3.3. Influence of the starting vanadium compound on the product phases

Influence of the starting vanadium compound on the product phases was examined using the reaction conditions of P/V = 2 at 315 °C (Table IV). Regardless of the starting vanadium compound having a valence state of vanadium between 3 and 5, Phase 2 was obtained. This may be rational, because during the glycothermal treatment vanadium is reduced to the vanadium(III) species (*vide supra*). In the case of NH_4VO_3, an unidentified product was obtained and this is left for further study.

3.4. Thermal analyses

3.4.1. Phase 1

Results of TG-DTA analyses in a nitrogen stream are shown in Fig. 2 and the XRD patterns of the products heat-treated at various temperatures are shown in Fig. 3. Gradual weight loss started around 300 °C and continued to 900 °C; about 10 wt% loss was observed up to 700 °C. The DTA trace showed no clear endo- or exothermic peak. The crystal structure of Phase 1 was preserved up to 500 °C. Phase 1 transformed to an unknown phase which is tentatively denoted as Phase M.

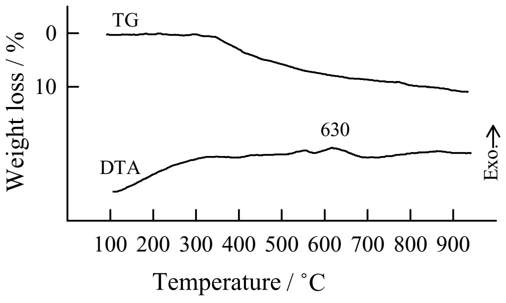

Figure 2 Thermal analysis of Phase 1 in N_2 stream.

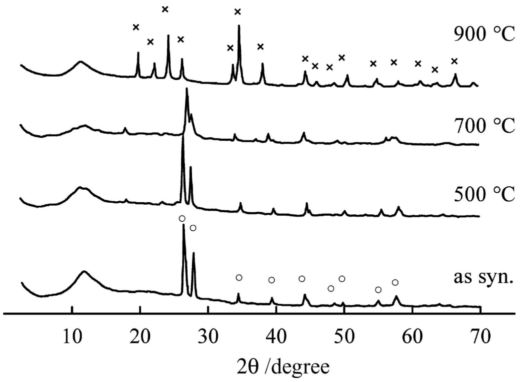

Figure 3 XRD patterns of Phase 1 treated at various temperatures in N_2 stream. (○; Phase 1, ×; VPO_4).

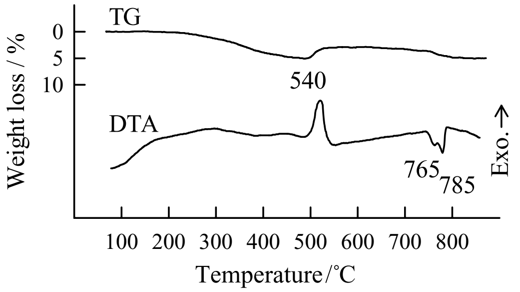

Figure 4 Thermal analysis of Phase 1 in the oxidative atmosphere ($3.8\%O_2$–$96.2\%N_2$).

The XRD pattern of Phase M resembled that of the product obtained by Hodnett and Delmon [25] by reduction of β-$VOPO_4$ in the hydrogen stream for 15 h. A broad exothermic peak observed at about 630 °C seems to correspond to the transformation from Phase 1 to Phase M. Phase M further transformed to VPO_4 by the heat treatment up to 900 °C.

Figs 4 and 5 show the TG-DTA traces of Phase 1 in the oxidative atmosphere of $3.8\%O_2$ in nitrogen and the XPD patterns of the products heat-treated in this oxidative stream at different temperatures, respectively. After gradual weight loss up to 500 °C, weight increase of about 3 wt% accompanying an exothermic peak was observed around 540 °C. The XRD patterns clearly indicated that the weight increase was due to the oxidation of Phase 1 to β-$VOPO_4$. The endothermic DTA peaks at around 770 °C correspond to fusion of β-$VOPO_4$. Vaughey et al. [20] reported that thermal decomposition of their tetragonal phase in nitrogen yielded a mixture of VPO_4 and V_2O_3, while aerobic decomposition gave a mixture of β-$VOPO_4$ and V_2O_5. On the contrary, thermal decomposition of the present product, Phase 1, did not give the vanadium oxide species.

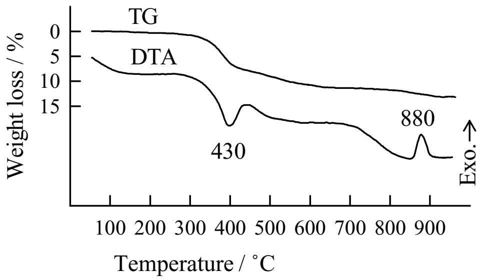

Figure 6 Thermal analysis of Phase 2 in N_2 stream.

3.4.2. Phase 2

Results for TG-DTA analyses of Phase 2 in the nitrogen stream are shown in Fig. 6 and the XRD patterns of the products heat-treated at various temperatures are shown in Fig. 7. The endothermic weight loss between 300 and 450 °C was about 8 wt% and the XRD pattern of the sample just after the endothermic peak (430 °C) was assigned to Phase 1. Therefore, it was concluded that the endothermic peak at 430 °C was due to desorption of water molecules and/or organic moieties, which was associated with formation of Phase 1 from Phase 2. Gradual weight loss continued to 650 °C, and the samples treated at 600 and 700 °C showed the XRD pattern of Phase M. At 880 °C, a slight weight loss was observed, which was accompanied with an exothermic peak. This exothermic peak was not detected in the case of Phase 1 (*vide supra*).

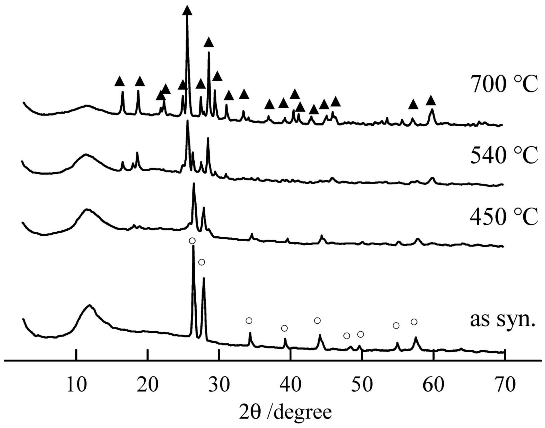

Figure 5 XRD patterns of Phase 1 treated at various temperatures in the oxidative atmosphere ($3.8\%O_2$–$96.2\%N_2$). (○; Phase 1, ▲; β-$VOPO_4$).

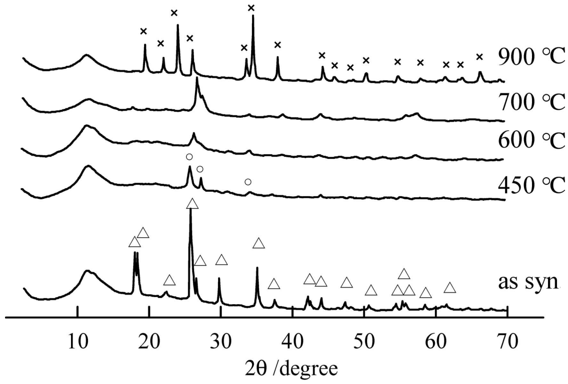

Figure 7 XRD patterns of Phase 2 treated at various temperatures in N_2 stream. (△; Phase 2, ○; Phase 1, ×; VPO_4).

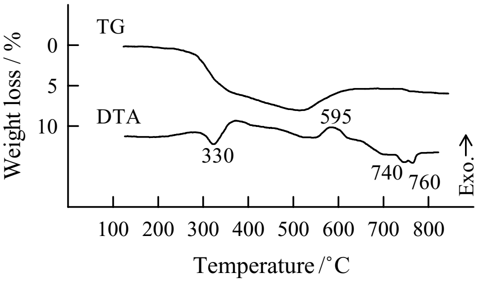

Figure 8 Thermal analysis of Phase 2 in the oxidative atmosphere (3.8%O_2–96.2%N_2).

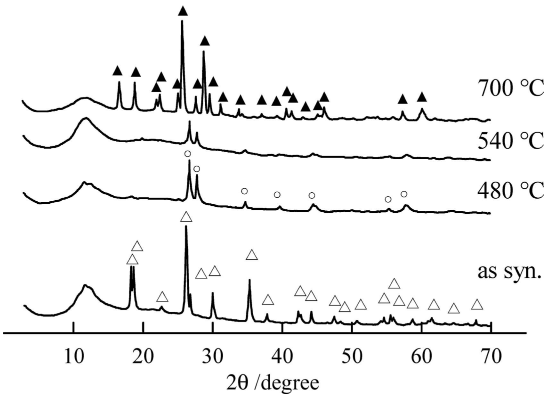

Figure 9 XRD patterns of Phase 2 treated at various temperatures in the oxidative atmosphere (3.8%O_2–96.2%N_2). (△; Phase 2, ○; Phase 1, ▲; β-$VOPO_4$)

At this moment we do not have any definite explanation to this, however, the difference in the free energy at the surface might be one reason. After the heat treatment at 900 °C, the XRD pattern of VPO_4 was observed, and the exothermic peak at 880 °C is attributed to crystallization to VPO_4. Total weight loss through these processes amounted to 12.6 wt%.

Fig. 8 shows TG-DTA analyses of Phase 2 in 3.8% O_2–nitrogen and the XRD patterns of the products heat-treated at various temperatures are shown in Fig. 9. At around 330 °C, a large weight loss accompanying an endothermic peak was observed and weight loss continued to 530 °C. The samples treated in this oxidative condition between 480 and 540 °C exhibited the XRD pattern of Phase 1. Therefore, at lower temperatures, essentially identical phase transformation took place in both aerobic and anaerobic conditions, although under the aerobic condition, the phase transformation from Phase 2 to Phase 1 occurred at a lower temperature. Thereafter, weight gain accompanying an exothermic peak was observed. The sample treated after 700 °C was revealed to be β-$VOPO_4$, and therefore, the weight gain at ∼595 °C is attributed to oxidation to β-$VOPO_4$. The endothermic peaks at around 750 °C were due to fusion of β-$VOPO_4$.

When Phase M, obtained by heat treatment of Phase 2 in nitrogen at 600 °C, was oxidized at the same temperature in 3.8% O_2–nitrogen, the product showed the XRD pattern of $(VO)_2P_2O_7$.

All the information in phase transformation is summarized in Fig. 10.

4. Discussion

Two vanadium(III) phosphate hydrate phases were prepared by the glycothermal reaction of various vanadium compounds with triethyl phosphate. Since the glycothermal condition is a severely reducing one [26, 27], vanadium compounds having higher oxidation states can be easily reduced to the trivalent vanadium species. The XRD patterns of these products were essentially identical with the reported tetragonal and monoclinic phases. So far, synthesis of vanadium(III) phosphate hydrates were carried out by hydrothermal reactions in the presence of organic amines or ammonium ions, and it was reported that the vanadium(III) phosphate hydrate phases were not crystallized in the absence of these compounds. Although the role of the organic ammines or ammonium ions has not been elucidated, the present paper clearly showed that vanadium(III) phosphate hydrates were crystallized without the aid of amine bases.

Although Phase 1 exhibited the essentially identical XRD pattern reported for tetragonal

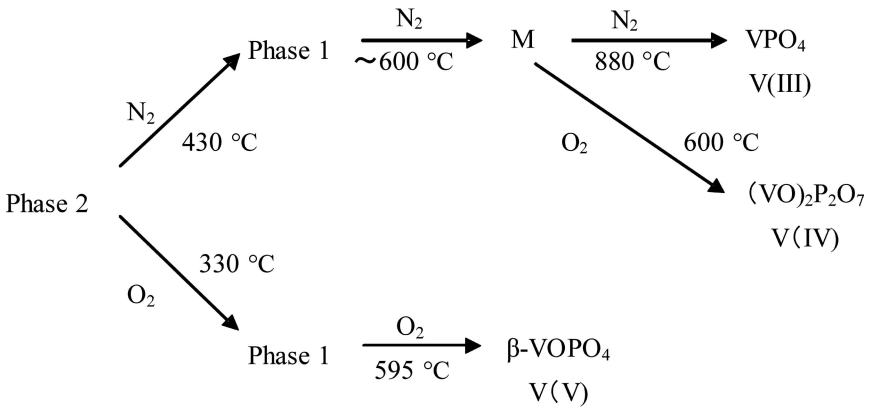

Figure 10 Transformation of Phase 1 and Phase 2.

$V_{1.23}(PO_4)(OH)_{0.69}(H_2O)_{0.31}\cdot 0.33H_2O$, our product seems to have a higher P/V ratio than the reported compounds had. The following results suggested this argument.

(1) Phase 2, $VPO_4\cdot H_2O$, transformed into Phase 1, which suggests that the two phases have the identical P/V ratio.

(2) The XRD patterns of the samples obtained by calcination of Phase 1 under anaerobic and aerobic conditions did not show any evidence for the formation of V_2O_3 and V_2O_5, respectively.

(3) Oxidation of vanadium-rich phase would cause the weight increase; Theoretical weight *increase* caused by oxidation of the $V_{1.23}(PO_4)(OH)_{0.69}(H_2O)_{0.31}\cdot 0.33H_2O$ phase to the mixture of $VOPO_4$ and V_2O_5 is 1.07%, and that from $V_{5.12}(PO_4)_4(OH)_{3.36}(H_2O)_{0.64}\cdot 0.84H_2O$ is 3.45%. On the other hand, oxidation of Phase 1 was accompanied with total 5% weight *decrease*.

The crystal structure of the tetragonal phase contains chains of face-sharing vanadium/oxygen octahedra in the *ab* plane. Two oxygen atoms of a phosphate group are incorporated into face-sharing octahedral chains, and the other two oxygen atoms of the phosphate group connect to the orthogonal chains of face-sharing vanadium/oxygen octahedra. Four octahedra share a common oxygen atom at the intersection of orthogonal chains [20]. Because of electrostatic repulsion between V(III) cations across the octahedral faces, the octahedral sites are only partially occupied with V(III) ions. Vaughey et al. [20] suggested that at the ideal composition, the vanadium cations occupy 2/3 of the sites in the face-sharing octahedral chain with an ordered arrangement in which each pair of vanadium cations share only one octahedron face (that is, the number of vanadium atom chain is 2). However, empirical formula for the phase suggests the statistical occupancies of the octahedra are 61.5% and 64% for $V_{1.23}(PO_4)(OH)_{0.69}(H_2O)_{0.31}\cdot 0.33H_2O$ and $V_{5.12}(PO_4)_4(OH)_{3.36}(H_2O)_{0.64}\cdot 0.84H_2O$, respectively. The average number of a vanadium atom chain corresponds to 1.6–1.8. In random distribution, a substantial fraction of the vanadium atoms are present as dimers but there is also a significant population of isolated octahedra (vertex-sharing chains of octahedra are formed). In an extreme case, vanadium ions would occupy one half of the octahedral sites of the face-sharing chain, which would give a hypothetical formula of $V_{1+x}(PO_4)(OH)_{3x}(H_2O)_{1-x}\cdot nH_2O$ $(x = 0)$.

The observed weight loss (12.6 wt%) of Phase 2 was larger than that (11.0 wt%) expected from the ideal formula of $VPO_4\cdot H_2O$. Since the weight decrease took place at relatively high temperature, this cannot be explained by desorption of physisorbed water. The IR spectra of Phase 2 (data not shown) indicated the presence of a small amount of organic moieties. Although the actual location of the organic moieties is not clear at this stage, these organic moieties seem to be strongly bound to the crystal, presumably to the surface of the crystal, by the covalent bondings. Similar occlusion of the organic amines in the $VPO_4\cdot H_2O$ phase was reported [28].

5. Conclusions

Glycothermal reaction of vanadium compounds with triethyl phosphate at 200–315 °C afforded tetragonal (Phase 1) and monoclinic (Phase 2) phases of vanadium phosphate hydrate. As far as we know, this is the first example of the formation of crystalline vanadium(III) phosphate hydrate without the aid of amine bases. The monoclinic phase (Phase 2) occluded organic moieties, while the tetragonal phase (Phase 1) had a higher P/V ratio than that of the previously-reported compounds. The monoclinic phase (Phase 2) transformed into the tetragonal phase (Phase 1) on heating.

References

1. T. YAMAGUCHI and H. YANAGIDA, in "Ceramics processing" (Gihoudou publishing, 1985).
2. S. SO-MIYA, in "New materials series-Hydrothermal reactions 1, 2" (Uchida-Roukakuho Publishing, 1986).
3. D. M. BIBBY and M. P. DALE, *Nature* (London) **317** (1985) 157.
4. M. C. CRUICKSHANK and L. S. DENT GLASSER, *Acta Cryst.* **C41** (1985) 1014.
5. M. INOUE, H. KOMINAMI and T. INUI, *J. Am. Ceram. Soc.* **73** (1990) 1100.
6. M. INOUE and T. INUI, *Adv. Sci. Technol.* **14** (1999) 41.
7. M. INOUE, *Adv. Sci. Technol.* **29** (2000) 855.
8. M. INOUE, *J. Phys: Condens. Matter* **16** (2004) S1291.
9. M. INOUE, Y. KONDO and T. INUI, *Inorg. Chem.* **27** (1988) 215.
10. M. INOUE, H. TANINO, Y. KONDO, T. INUI, *J. Am. Ceram. Soc.* **72** (1989) 352.
11. M. INOUE, H. OTSU, H. KOMINAMI and T. INUI, *J. Am. Ceram. Soc.* **74** (1991) 1452.
12. M. INOUE, H. OTSU, H. KOMINAMI and T. INUI, *J. Alloys. Compd.* **226** (1995) 146.
13. M. INOUE, H. KOMINAMI and T. INUI, *J. Chem. Soc. Dalton Trans.* 3331 (1991).
14. G. CENTI, F. TRIFIRÒ, J. R. EBNER and V. M. FRANCHETTI, *Chem. Rev.* **88** (1988) 55.
15. H. IGARASHI, K. TSUJI, T. OKUHARA and M. MISONO, *J. Phys. Chem.* **97** (1993) 7065.
16. G. BUSCA, F. CAVANI, G. CENTI and F. TRIFIRO, *J. Catal.* **99** (1986) 400.
17. T. MIYAKE and T. DOI, in "3rd World Congress on Oxidation Catalysis", R. K. GRASSELLI, S. T. OYAMA, A. M. GAFFNEY, J. E. LYONS (eds.), (Elsevier Science B. V., 1997), p 835.
18. G. LADWIG, K. H. JOST, K. SCHLESINGER, *Z. Chem.* **19** (1979) 386.
19. B. TOFIELD, G. R. CRANE, G. PASTUER and R. SHERWOOD, *J. Chem. Soc. Dalton Trans.* (1975) 1806.
20. J. T. VAUGHEY, W. T. A. HARRISON, A. J. JACOBSON, D. P. GOSHORN and J. W. JOHNSON, *Inorg. Chem.* **33** (1994) 2481.
21. M. SCHINDLER, W. JOSWIG and W. H. BAUR, *Eur. J. Solid State Inorg. Chem.* **32** (1995) 109.
22. A. EL BADRAOUI, J. Y. PIVAN, M. MAUNAYE, M. LOUËR and D. LOUËR, *J. Alloys Comp.* **245** (1996) 47.
23. B. K. HODNETT, PH. PERMANNE and B. DELMON, *Appl. Catal.* **6** (1983) 231.

24. M. SCHINDLER, W. JOSWIG and W. H. BAUR, *Eur. J. Solid State Inorg. Chem.* **32** (1995) 109.
25. B. K. HODNETT and B. DELMON, *Appl. Catal.* **6** (1983) 245.
26. M. INOUE, *Adv. Sci. Technol.* **31** (2003) 511.
27. M. FIGLARZ, F. FIEVET, J. P. LAGIER, Internat. Meeting on Advanced Materials, Tokyo, May 30 to June 3, 1988, C5.1.
28. S. C. LIM, J. T. VAUGHEY, W. T. A. HARRISON, L. L. DUSSACK, A. J. JACOBSON and J. W. JOHNSON, *Solid State Ionics* **84** (1996) 219.

Received 11 November 2004
and accepted 13 September 2005